

Journal of Materials Chemistry C

Accepted Manuscript



This is an *Accepted Manuscript*, which has been through the Royal Society of Chemistry peer review process and has been accepted for publication.

Accepted Manuscripts are published online shortly after acceptance, before technical editing, formatting and proof reading. Using this free service, authors can make their results available to the community, in citable form, before we publish the edited article. We will replace this *Accepted Manuscript* with the edited and formatted *Advance Article* as soon as it is available.

You can find more information about *Accepted Manuscripts* in the [Information for Authors](#).

Please note that technical editing may introduce minor changes to the text and/or graphics, which may alter content. The journal's standard [Terms & Conditions](#) and the [Ethical guidelines](#) still apply. In no event shall the Royal Society of Chemistry be held responsible for any errors or omissions in this *Accepted Manuscript* or any consequences arising from the use of any information it contains.

ARTICLE

A Brilliant Cryogenic Magnetic Coolant. Magnetic and Magnetocaloric Study of the Ferromagnetically Coupled GdF_3^\dagger

Cite this: DOI: 10.1039/x0xx00000x

Received 00th January 2012,
Accepted 00th January 2012

DOI: 10.1039/x0xx00000x

www.rsc.org/

Yan-Cong Chen,^a Jan Prokleška,^b Wei-Jian Xu,^a Jun-Liang Liu,^a Jiang Liu,^a
Wei-Xiong Zhang,^a Jian-Hua Jia,^{*a} Vladimír Sechovský^b and Ming-Liang Tong^{*a}

The use of paramagnetic molecules as cryogenic coolants usually requires relatively large fields to obtain a practical cooling effect. Thus, research for magnetic molecular materials with larger MCEs in fields of ≤ 2 T is the central science. In this work, the crystal structure, magnetic susceptibility and isothermal magnetization for inorganic framework material GdF_3 were measured, and the isothermal entropy change was evaluated up to 9 T. Thanks to combination of the large isotropic spin of Gd^{3+} , the dense structure and the weak ferromagnetic interaction, an extremely large $-\Delta S_m$ for GdF_3 was observed up to $528 \text{ mJ cm}^{-3} \text{ K}^{-1}$ for $\Delta\mu_0 H = 9$ T, proving itself to be an exceptional cryogenic magnetic coolant.

Introduction

The magnetocaloric effect (MCE) was discovered in 1881 in metallic iron by Warburg,¹ and the magnetic refrigeration soon become a powerful technique to obtain and maintain ultra-low temperature by adiabatic demagnetization (ADR).²⁻³ At an early stage, the cryogenic magnetic coolants are mainly the inorganic paramagnetic salts and oxides, such as $\text{Gd}_2(\text{SO}_4)_3 \cdot 8\text{H}_2\text{O}$ and $\text{Gd}_3\text{Ga}_5\text{O}_{12}$ (GGG).⁴ In recent years, molecular materials suddenly emerged in this field as an unprecedented classification, and a lot of highly competitive molecular magnetic coolants of 3d,⁵⁻¹¹ 3d-4f¹²⁻²¹ and 4f-types²²⁻²⁹ have been synthesized and characterized. Their distinct advantages, such as stoichiometric composition, monodispersity and modifiability, have provided the researchers a perfect platform to realize the design strategies towards cryogenic magnetic coolants. Various lessons have been learned and proved, including but not limited to the large spin state, low anisotropy, weak interaction and large metal-to-ligand ratio.³⁰⁻³⁵

For the best cooling performance around liquid helium temperature, it is believed that the Gd^{3+} ion is a wonderful choice owing to the half-filled 4f orbital ($S = 7/2$), magnetic isotropy and usually weak exchange interactions. Additionally, the low magnetic ordering temperature can still be maintained even with high metal-to-ligand ratio, and a large MCE can be obtained, especially with volumetric units.³⁶⁻³⁷ Soon after, the competition in molecular magnetic coolants became the race on the reduction of counterions accompanying Gd^{3+} . To date, many gadolinium carboxylates including acetates, formats and oxalates have been reported, with increasing MCE chasing after GGG.³⁸⁻⁴²

Since there is little room for the organic ligands to keep shrinking, the most recent focus in this field dramatically returned to the inorganic compounds based on small counterions such as OH^- , SO_4^{2-} , O^{2-} .⁴³⁻⁴⁵ Following the strategies learned in molecular systems,³⁰⁻³⁵ significant enhancement of MCE in these inorganic compounds have been observed, and the orthorhombic $\text{Gd}(\text{OH})\text{CO}_3$ finally surpass the performance of GGG and set a new record.⁴⁶ However, the story seems not over yet as a better example of GdPO_4 was reported just after half a year.⁴⁷

In the inorganic area, the utilization of the aforementioned strategies must be more careful, because strong magnetic interactions are more likely to exist, thus hinder the MCE. Compared with relatively versatile magnetic interaction transmitted by the OH^- , SO_4^{2-} , O^{2-} bridges, weak ferromagnetic coupling transmitted by bent $\mu\text{-F}^-$ bridges is often observed in lanthanide complexes,⁴⁸⁻⁴⁹ which urge us to investigate the MCE performance of gadolinium fluoride. Although GdF_3 was tested as the working material for a toroidal ADR prototype,⁵⁰ the presence of Gd_2O_3 impurity prevented the intrinsic magnetocaloric performance of GdF_3 from unrevealing. Herein we report the detailed magnetic and magnetocaloric study on the pure sample of GdF_3 . The occurrence of ferromagnetic coupling and extremely large MCE proves it to be the best cryogenic magnetic coolant ever reported.

Experimental section

Synthesis of GdF_3

Pure polycrystalline GdF_3 can be hydrothermally synthesized using analytical reagent ($> 99.9\%$) of aqueous GdCl_3 and excess amount of NaBF_4 or NH_4F , while commercial product is also available.

X-ray Crystallography

The X-ray powder diffraction data for structure refinement was collected on Bruker D8 Advance with Cu K_{α} X-ray radiation (40 kV, 40 mA). The step-scanned X-ray powder diffraction data was recorded in the 2θ range of 20 – 115° with 0.02° 2θ step and 8 seconds/step scan speed. The structural model of TbF_3 (in space group $Pnma$) was used as the initial structural models for Rietveld refinement, which was carried on Reflex Powder Refinement module of Material Studio. The structural parameters, together with Pseudo-Voigt profile parameters, background parameters, the cell constants, the zero point of the diffraction pattern, the Berar-Baldinozzi asymmetry correction parameters and the March-Dollase preferred orientation correction parameters, were optimized step by step to improve the agreement between the calculated and the experimental powder diffraction pattern. The final Rietveld refinement plot is shown in Fig. S1. Further details on the crystal structure may be obtained in the ESI (Tables S1 and S2) and from the Fachinformationszentrum Karlsruhe, 76344 Eggenstein-Leopoldshafen, Germany (fax: (+49) 7247-808-666; e-mail: crysdata@fiz-karlsruhe.de), by quoting the depository number CSD-429920 (GdF_3).

Physical Measurements

Magnetic measurements were performed on polycrystalline sample of GdF_3 using a Quantum Design PPMS with VSM option. Variable-temperature magnetic susceptibility measurement was performed on polycrystalline sample in an applied dc field of 0.1 T between 2 ~ 300 K, and the isothermal magnetization were measured from 2 K to 10 K in an applied dc field up to 9 T. Diamagnetic correction was applied based on the Pascal's constant. Low-temperature specific heat was studied on a Quantum Design PPMS up to 9 T with the 3He option adopting standard relaxation technique.

Table 1 Crystal Data and Structural Refinement for GdF_3 .

Chemical formula	GdF_3
Formula Mass / $g\ mol^{-1}$	214.25
Crystal system	Orthorhombic
Space group	$Pnma$
Z	4
$a/\text{\AA}$	6.5718(1)
$b/\text{\AA}$	6.9844(1)
$c/\text{\AA}$	4.3903(1)
Unit cell volume/ \AA^3	201.21
$\rho_{\text{calcd}} / g\ cm^{-3}$	7.062
R_p	1.62%
R_{wp}	2.21%

Results and discussion

Crystal Structure

Although the powder X-ray diffraction pattern of GdF_3 was listed in JCPDF #49-1804, the exact crystal structure has not been determined. Here by the Rietveld refinement on the Powder X-ray diffraction pattern (Figure S1), it is found that GdF_3 crystallizes in the orthorhombic space group $Pnma$ and shares the same structure for SmF_3 , EuF_3 , TbF_3 , HoF_3 and YbF_3 (Table 1). In the crystal structure, each Gd^{3+} ion is 9-coordinated in a tricapped trigonal prismatic geometry (Figure 1), while each F^- ion is μ_3 -bridging, just corresponding to the stoichiometric ratio 1:3. The lengths of Gd-F bonds are

generally similar, ranging from 2.331 to 2.501 \AA , while the Gd-F-Gd angles are quite different, lying between 98.88° and 139.03° . The nearest Gd...Gd separations are 3.672 \AA , which form a series of zigzag chains along the a axis and then further extended into a 3-dimensional framework (Figure 1 and Figure S2). Thanks to the simple composition, the formula mass of GdF_3 is only $214.25\ g\ mol^{-1}$, trapping as much as 73.4% of Gd^{3+} in an extremely dense structure with $\rho = 7.062\ g\ cm^{-3}$. Therefore, GdF_3 shall be a wonderful magnetic coolant so long as there isn't long-range antiferromagnetic ordering in the working temperature region.

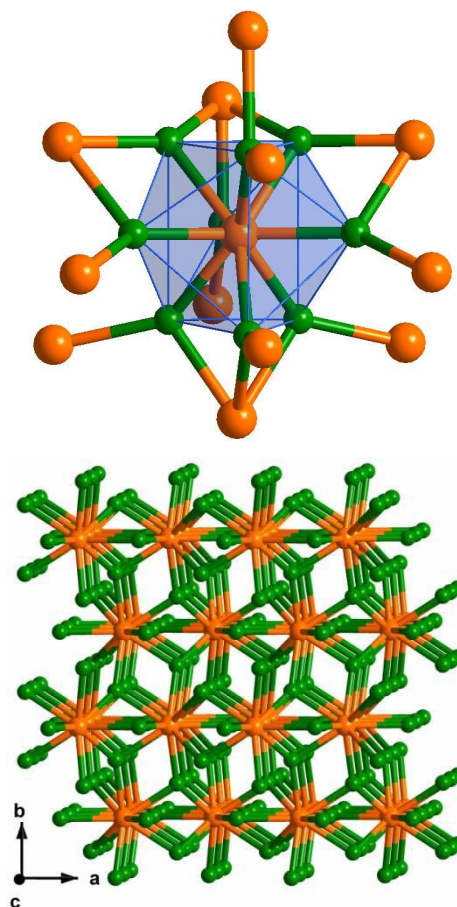


Figure 1 The crystal structure of GdF_3 . Top: The coordination environment of Gd^{3+} ; Down: The extended framework of GdF_3 viewed along the c axis. Colour Codes: Gd, orange; F, green.

Magnetic Properties

Variable-temperature magnetic susceptibility measurement was performed on polycrystalline sample of GdF_3 in an applied dc field of 0.1 T (Figure 2). At room temperature, the $\chi_m T$ value is $7.96\ cm^3\ K\ mol^{-1}$, slightly larger than the spin-only value expected for a free Gd^{3+} ion with $g = 2$ ($7.875\ cm^3\ K\ mol^{-1}$). Upon cooling, $\chi_m T$ keeps increasing to $11.2\ cm^3\ K\ mol^{-1}$ at 2 K, suggesting dominant ferromagnetic interactions between Gd^{3+} ions. The inverse magnetic susceptibility ($1/\chi_m$) obeys the Curie-Weiss law with $C = 7.91\ cm^3\ K\ mol^{-1}$ and $\theta = +0.7\ K$. No sign of the long-range magnetic ordering can be observed above

2 K, as the ordering temperature is reported to be around 1.25 K.⁵¹ Such a behaviour is extremely favourable for a large cryogenic MCE, and it is quite different from those complexes with hydroxide bridges, where strong antiferromagnetic interactions are common and usually harm the full utilization of the MCE. The ferromagnetic coupling in GdF₃ and the low ordering temperature rule out our last worry about its capability as a promising cryogenic magnetic coolant.

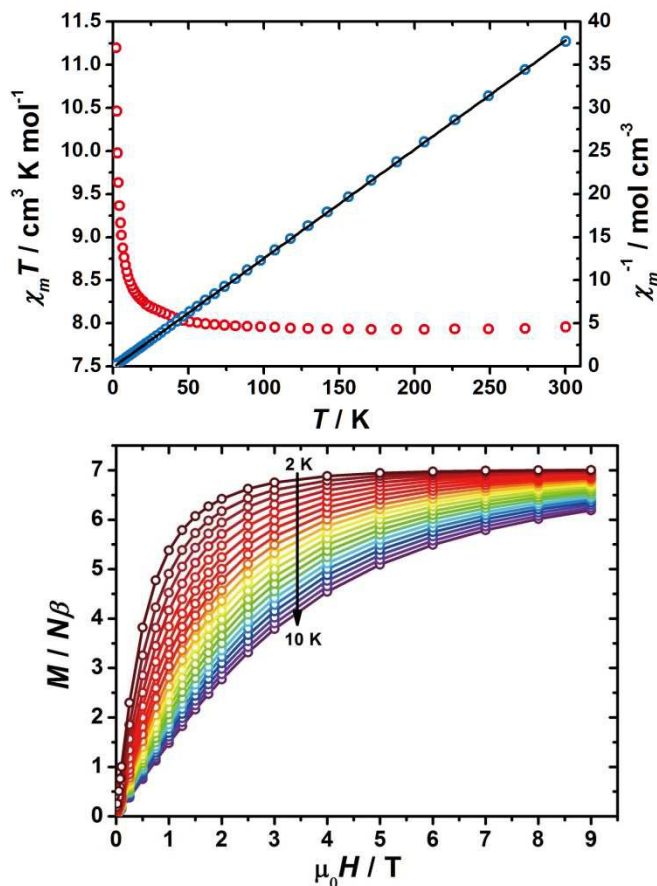


Figure 2 Magnetic Properties of GdF₃. Left: Temperature-dependencies of the magnetic susceptibility product ($\chi_m T$) and inverse magnetic susceptibility ($1/\chi_m$) at 2–300 K with a dc field of 0.1 T. Right: Magnetization *versus* the dc field in the temperature range of 2–10 K. The black solid line represents the least-square fit for the Curie-Weiss law.

To calculate the precise value of $-\Delta S_m$, the isothermal magnetization for GdF₃ were measured from 2 K to 10 K in an applied dc field up to 9 T (**Figure 2**). The magnetization increases quickly with the applied field below 2 T and reaches the saturation value of $7.0 N\beta$ at 2 K and 9 T, which is in good agreement with the expected value for a Gd³⁺ ion ($s = 7/2$, $g = 2$).

The isothermal entropy change can be calculated by applying the Maxwell equation:

$$\Delta S_m(T) = \int_0^H \left[\frac{\partial M(T, H)}{\partial T} \right]_H dH$$

Just as many reported ferromagnetic coupling systems, the maximum $-\Delta S_m$ values for GdF₃ grow rapidly with increasing ΔH , namely $181 \text{ mJ cm}^{-3} \text{ K}^{-1}$, $321 \text{ mJ cm}^{-3} \text{ K}^{-1}$ and $399 \text{ mJ cm}^{-3} \text{ K}^{-1}$ for

$\Delta\mu_0 H = 1 \text{ T}$, 2 T and 3 T, respectively (**Figure 3**). For larger ΔH , the increase of $-\Delta S_m$ values become slower, reaching $474 \text{ mJ cm}^{-3} \text{ K}^{-1}$ and $506 \text{ mJ cm}^{-3} \text{ K}^{-1}$ for $\Delta\mu_0 H = 5 \text{ T}$ and 7 T, and the peaks of $-\Delta S_m$ *versus* T curves gradually shift to higher temperatures. These results are in line with the heat capacity tests for the toroidal ADR prototype,⁵¹ and the maximum value here we obtained is $528 \text{ mJ cm}^{-3} \text{ K}^{-1}$ ($74.8 \text{ J kg}^{-1} \text{ K}^{-1}$) at $T = 3.2 \text{ K}$ and $\Delta\mu_0 H = 9 \text{ T}$, close to the theoretical limiting value of $570 \text{ mJ cm}^{-3} \text{ K}^{-1}$ ($80.7 \text{ J kg}^{-1} \text{ K}^{-1}$) calculated from $R \ln(2s+1)/Mw$ with $s = 7/2$ and $Mw = 214.25 \text{ g mol}^{-1}$.

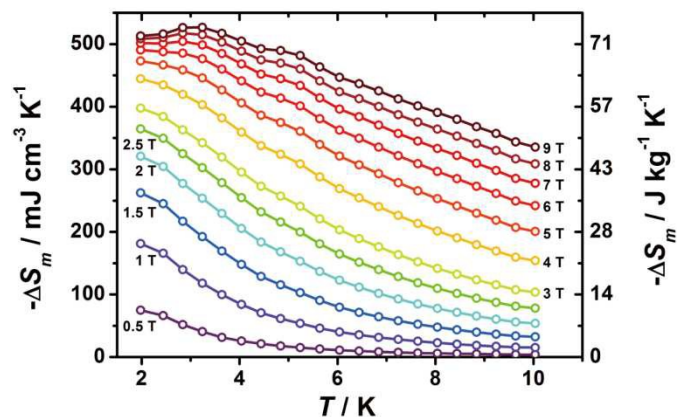


Figure 3 Temperature-dependencies of $-\Delta S_m$ for selected values of $\Delta\mu_0 H$ obtained from magnetization data. The data with field variation below 0.5 T are omitted for clarity.

Heat Capacity

The low temperature heat capacity (C) measurements were also performed to further investigate the MCE of GdF₃ (**Figure 4**), and no peak around 3.8 K corresponding to Gd₂O₃ can be found.⁵⁰ The curves shows typical trends as most cryogenic magnetic coolants, with the higher temperature region attributed to the lattice contribution and the lower part dominated by Schottky type magnetic contribution. The lattice one, C_{latt} , can be fitted to the Debye's model and yield a high Debye temperature (θ_D) of 284(3) K with $\nu_D = 4$, indicating a rigid crystal framework that is favourable to large MCE. A λ -shaped anomaly is observed in the zero field at approximately 1.21 K but suppressed by applied fields, indicating the emergence of a magnetic phase transition in good agreement with the reported 1.25 K.⁵¹

Then, the entropy can be obtained by numerical integration from the experimental C , using:

$$S(T) = \int_0^T C(T)/T dT$$

with a constant value base on the high temperature saturation value of magnetic entropy ($S_{m, \text{sat}} = R \ln(2s+1) = 2.08 R$) added to the low-field entropy to compensate for experimental inaccessibility to absolute zero. From the heat capacity, the maximal isothermal magnetic entropy changes (ΔS_m) were obtained as $186 \text{ mJ cm}^{-3} \text{ K}^{-1}$, $395 \text{ mJ cm}^{-3} \text{ K}^{-1}$ and $473 \text{ mJ cm}^{-3} \text{ K}^{-1}$ for $\Delta\mu_0 H = 1 \text{ T}$, 3 T and 5 T, respectively, in great agreement with the results calculated from the magnetization (**Figure 5**). These are accompanied by the large adiabatic temperature change (ΔT_{ad}) up to 17 K for $\Delta\mu_0 H = 5 \text{ T}$ (**Figure**

S3), highlighting the competitiveness of GdF_3 as a brilliant cryogenic magnetic coolant.

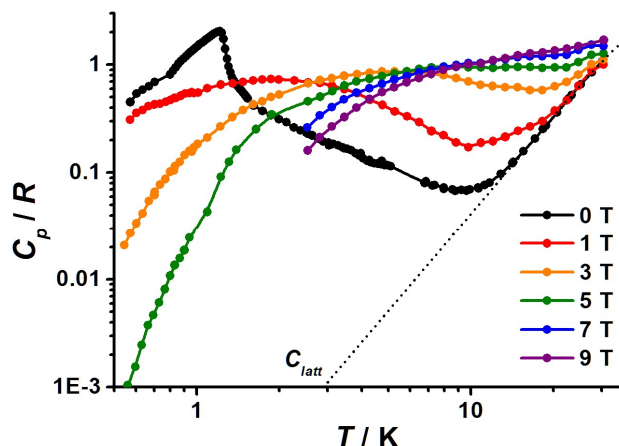


Figure 4 Temperature-dependencies of the heat capacity normalized to the gas constant in selected applied fields. The dotted line represents the lattice contribution.

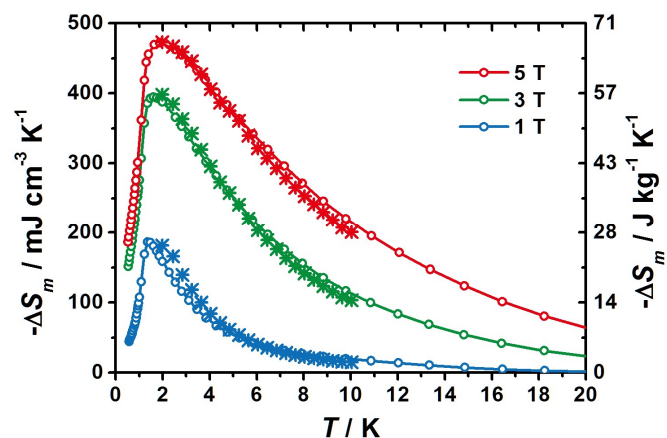


Figure 5 Temperature-dependencies of $-\Delta S_m$ obtained from magnetization (★) and heat capacity (●) for selected $\Delta\mu_0 H$.

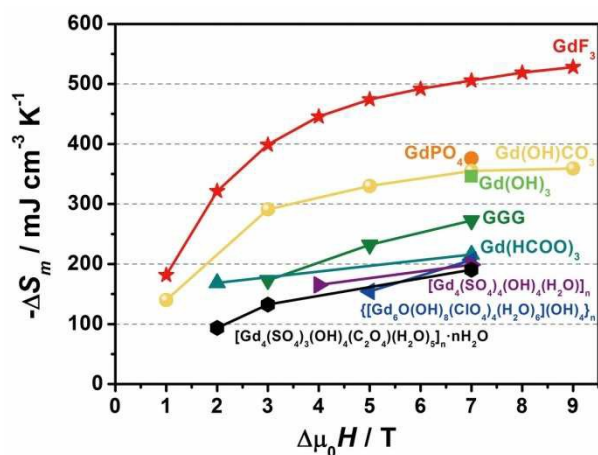


Figure 6 The maximum reported $-\Delta S_m$ value versus the corresponding $\Delta\mu_0 H$ for selected cryogenic magnetic coolants.

Conclusions

The area of cryogenic magnetic coolants is full of competitions, and there has never been a candidate that can hold the record for a long time. Thanks to such competition in a sense, researchers are now much wiser at adopting suitable strategies for the design of high performance magnetic coolants. Although the record set by $\text{Gd}(\text{OH})\text{CO}_3$ ⁴⁶ has been taken recently, we haven't stopped seeking and finally present the ferromagnetically coupled GdF_3 .

As demonstrated in **Figure 6** and **Table 2**, the other cryogenic magnetic coolant with $-\Delta S_m$ larger than $400 \text{ mJ cm}^{-3} \text{ K}^{-1}$ has never been reported, while the maximum value for GdF_3 has already exceeded $500 \text{ mJ cm}^{-3} \text{ K}^{-1}$. Comparing the $-\Delta S_m$ with $\Delta\mu_0 H = 7 \text{ T}$ for the sake of fairness, the performance of GdF_3 ($506 \text{ mJ cm}^{-3} \text{ K}^{-1}$) surpass that of GdPO_4 ($375.8 \text{ mJ cm}^{-3} \text{ K}^{-1}$)⁴⁷ by 34.6%, setting a new record. Last but not least, the dense structure and ferromagnetic interaction in GdF_3 leads to still excellent performance even for lower $\Delta\mu_0 H$ such as 2 T and 1 T, highlighting the competitiveness.

Table 2. Magnetic entropy change for selected molecule-based materials.

Complex ^{ref}	$\Delta\mu_0 H$ (T)	$-\Delta S_{m, \max}$ ($\text{J kg}^{-1} \text{ K}^{-1}$)	$-\Delta S_m$ ($\text{mJ cm}^{-3} \text{ K}^{-1}$)
$[\text{Gd}_4(\text{SO}_4)_3(\text{OH})_4(\text{C}_2\text{O}_4)(\text{H}_2\text{O})_5]_n \cdot n\text{H}_2\text{O}$ ⁴⁵	7	51.5	190
$[\text{Gd}_4(\text{SO}_4)_4(\text{OH})_4(\text{H}_2\text{O})]_n$ ⁴⁴	7	51.3	199
$\{[\text{Gd}_6\text{O}(\text{OH})_8(\text{ClO}_4)_4(\text{H}_2\text{O})_6](\text{O}(\text{H})_4)_n\}$ ⁴³	7	46.6	207
$\text{Gd}(\text{HCOO})_3$ ⁴¹	7	55.9	216
$\text{Gd}_3\text{Ga}_5\text{O}_{12}$ (GGG) ⁴	7	38.4	272
$\text{Gd}(\text{OH})_3$ ⁵²	7	62.0	346
$\text{Gd}(\text{OH})\text{CO}_3$ ⁴⁶	7	66.4	355
GdPO_4 ⁴⁷	7	62.0	376
GdF_3 (This work)	2	45.5	321
	5	67.1	474
	7	71.6	506

At this point, we believe the long journey in pursuit of the best cooling performance is close to the extreme. There is limited room, if any, for the further increase of the $-\Delta S_m$ value itself for Gd-based materials: some other compounds like GdOF , GdOOH , GdBO_3 and $\text{Gd}_2(\text{CO}_3)_3$ might worth some try, while Gd_2O_3 and $\text{Gd}(\text{OH})_3$ ⁵² are already known as antiferromagnets and suffer severe decrease of the full entropy. Future study on the cryogenic MCE shall turn the focus onto the other parameters such as ΔT_{ad} , cooling power and even production cost, where the Mn-based materials become strong competitors.¹¹ Although we have to admit that the coordination complexes with organic ligands can never be so comparative with inorganic complexes in such sense, it should not be forgotten that the ambitions of molecular materials have never been just about the value. We have witnessed how the numerous complexes seems useless can be rationally modified into good candidates for magnetic coolants, and we have been continuously learning about the magneto-structural correlations during the design and synthesis of these complexes. Furthermore, chemists' powerful skill on material engineering can still modify the behaviour of the inorganic compounds in the limitless nanomaterial and organic-inorganic

hybrid material, where the magnetic interaction, ordering temperature and low-field performance may be fine-tuned and optimized. *It is, perhaps, the end of the beginning.*

Acknowledgements

This work was supported by the “973 Project” (2012CB821704 and 2014CB845602), project NSFC (Grant no. 91122032, 21371183, 21121061 and 21201137), the NSF of Guangdong (S2013020013002), Program for Changjiang Scholars and Innovative Research Team in University of China (IRT1298). Part of the thermodynamic studies was performed in MLTL (<http://mltl.eu/>), which is supported within the program of Czech Research Infrastructures (project no. LM2011025).

Notes and references

^aKey Laboratory of Bioinorganic and Synthetic Chemistry of Ministry of Education, School of Chemistry & Chemical Engineering, Sun Yat-Sen University, Guangzhou, 510275, China. E-mail: tongml@mail.sysu.edu.cn

^bFaculty of Mathematics and Physics, Department of Condensed Matter Physics, Charles University, Ke Karlovu 5, CZ-12116 Prague 2, Czech Republic.

† Electronic Supplementary Information (ESI) available: Additional crystallography tables and figures of magnetic properties. See DOI: 10.1039/b000000x/

- 1 E. Warburg, *Ann. Phys.*, 1881, **249**, 141.
- 2 P. Debye, *Ann. Phys.*, 1926, **386**, 1154.
- 3 W. F. Giaouque, *J. Am. Chem. Soc.*, 1927, **49**, 1864.
- 4 B. Baudun, R. Lagnier and B. Salce, *J. Magn. Magn. Mater.*, 1982, **27**, 315.
- 5 M. Manoli, R. D. L. Johnstone, S. Parsons, M. Murrie, M. Affronte, M. Evangelisti and E. K. Brechin, *Angew. Chem Int. Ed.*, 2007, **119**, 4540.
- 6 M. Manoli, A. Collins, S. Parsons, A. Candini, M. Evangelisti and E. K. Brechin, *J. Am. Chem. Soc.*, 2008, **130**, 11129.
- 7 S. Nayak, M. Evangelisti, A. K. Powell and J. Reedijk, *Chem. Eur. J.*, 2010, **16**, 12865.
- 8 J.-P. Zhao, R. Zhao, Q. Yang, B.-W. Hu, F.-C. Liu and X.-H. Bu, *Dalton Trans.*, 2013, **42**, 14509.
- 9 R. Shaw, R. H. Laye, L. F. Jones, D. M. Low, C. Talbot-Eeckelaers, Q. Wei, C. J. Milios, S. Teat, M. Helliwell, J. Raftery, M. Evangelisti, M. Affronte, D. Collison, E.K. Brechin and E. J. L. McInnes, *Inorg. Chem.*, 2007, **46**, 4968.
- 10 C.-B. Tian, R.-P. Chen, C. He, W.-J. Li, Q. Wei, X.-D. Zhang and S.-W. Du, *Chem. Commun.*, 2014, **50**, 1915.
- 11 Y.-C. Chen, J.-L. Liu, J.-D. Leng, F.-S. Guo, P. Vrábel, M. Orendáč, J. Prokleška, V. Sechovský and M.-L. Tong, *Chem. Eur. J.*, 2014, **20**, 3029.
- 12 G. Karotsis, M. Evangelisti, S. J. Dalgarno and E. K. Brechin, *Angew. Chem. Int. Ed.*, 2009, **48**, 9928.
- 13 G. Karotsis, S. Kennedy, S. J. Teat, C. M. Beavers, D. A. Fowler, J. J. Morales, M. Evangelisti, S. J. Dalgarno and E. K. Brechin, *J. Am. Chem. Soc.*, 2010, **132**, 12983.
- 14 S. K. Langley, N. F. Chilton, B. Moubaraki, T. Hooper, E. K. Brechin, M. Evangelisti and K. S. Murray, *Chem. Sci.*, 2011, **2**, 1166.
- 15 Y.-Z. Zheng, M. Evangelisti and R. E. P. Winpenny, *Angew. Chem. Int. Ed.*, 2011, **50**, 3692.
- 16 J.-B. Peng, Q.-C. Zhang, X.-J. Kong, Y.-P. Ren, L.-S. Long, R.-B. Huang, L.-S. Zheng and Z. Zheng, *Angew. Chem. Int. Ed.*, 2011, **50**, 10649.
- 17 T. N. Hooper, J. Schnack, S. Piligkos, M. Evangelisti and E. K. Brechin, *Angew. Chem. Int. Ed.*, 2012, **51**, 4633.
- 18 Y.-Z. Zheng, M. Evangelisti, F. Tuna and R. E. P. Winpenny, *J. Am. Chem. Soc.*, 2012, **134**, 1057.
- 19 J.-B. Peng, Q.-C. Zhang, X.-J. Kong, Y.-Z. Zheng, Y.-P. Ren, L.-S. Long, R.-B. Huang, L.-S. Zheng and Z. Zheng, *J. Am. Chem. Soc.*, 2012, **134**, 3314.
- 20 E. M. Pineda, F. Tuna, R. G. Pritchard, A. C. Regan, R. E. P. Winpenny and E. J. L. McInnes, *Chem. Commun.*, 2013, **49**, 3522.
- 21 F.-S. Guo, Y.-C. Chen, J.-L. Liu, J.-D. Leng, Z.-S. Meng, P. Vrábel, M. Orendáč and M.-L. Tong, *Chem. Commun.*, 2012, **48**, 12219.
- 22 R. J. Blagg, F. Tuna, E. J. L. McInnes and R. E. P. Winpenny, *Chem. Commun.* 2011, **47**, 10587.
- 23 R. Sibille, T. Mazet, B. Malaman and M. François, *Chem. Eur. J.*, 2012, **18**, 12970.
- 24 M. Wu, F. Jiang, X. Kong, D. Yuan, L. Long, S. A. Al-Thabaiti and M. Hong, *Chem. Sci.*, 2013, **4**, 3104.
- 25 J.-M. Jia, S.-J. Liu, Y. Cui, S.-D. Han, T.-L. Hu and X.-H. Bu, *Cryst. Growth Des.* 2013, **13**, 4631.
- 26 S. Biswas, A. Adhikary, S. Goswami and S. Konar, *Dalton Trans.*, 2013, **42**, 13331.
- 27 L.-X. Chang, G. Xiong, L. Wang, P. Cheng and B. Zhao, *Chem. Commun.*, 2013, **49**, 1055.
- 28 Y.-C. Chen, F.-S. Guo, Y.-Z. Zheng, J.-L. Liu, J.-D. Leng, R. Tarasenko, M. Orendáč, J. Prokleška, V. Sechovský and M.-L. Tong, *Chem. Eur. J.*, 2013, **19**, 13504.
- 29 F.-S. Guo, Y.-C. Chen, L.-L. Mao, W.-Q. Lin, J.-D. Leng, R. Tarasenko, M. Orendáč, J. Prokleška, V. Sechovský and M.-L. Tong, *Chem. Eur. J.*, 2013, **19**, 14876.
- 30 Yu. I. Spichkin, A. K. Zvezdin, S. P. Gubin, A. S. Mischenko and A. M. Tishin, *J. Phys. D*, 2001, **34**, 1162.
- 31 M. Evangelisti and E. K. Brechin, *Dalton Trans.*, 2010, **39**, 4672.
- 32 R. Sessoli, *Angew. Chem. Int. Ed.*, 2012, **51**, 43.
- 33 J. W. Sharples and D. Collison, *Polyhedron.*, 2013, **54**, 91.
- 34 Y.-Z. Zheng, G.-J. Zhou, Z. Zheng and R. E. P. Winpenny, *Chem. Soc. Rev.*, 2013, **43**, 1462.
- 35 J.-L. Liu, Y.-C. Chen, F.-S. Guo and M.-L. Tong, *Coord. Chem. Rev.*, 2014, **281**, 26.
- 36 K. A. Gschneidner, Jr., V. K. Pecharsky, *Annu. Rev. Mater. Sci.*, 2000, **30**, 387.
- 37 K. A. Gschneidner, Jr., V. K. Pecharsky and A. O. Tsokol, *Rep. Prog. Phys.*, 2005, **68**, 1479.
- 38 M. Evangelisti, O. Roubeau, E. Palacios, A. Camín, T. N. Hooper, E. K. Brechin and J. J. Alonso, *Angew. Chem. Int. Ed.*, 2011, **50**, 6606.
- 39 F.-S. Guo, J.-D. Leng, J.-L. Liu, Z.-S. Meng and M.-L. Tong, *Inorg. Chem.*, 2012, **51**, 405.
- 40 G. Lorusso, M. A. Palacios, G. S. Nichol, E. K. Brechin, O. Roubeau and M. Evangelisti, *Chem. Commun.*, 2012, **48**, 7592.
- 41 G. Lorusso, J. W. Sharples, E. Palacios, O. Roubeau, E. K. Brechin, R. Sessoli, A. Rossin, F. Tuna, E. J. L. McInnes, D. Collison and M. Evangelisti, *Adv. Mater.*, 2013, **25**, 4653.

- 42 R. Sibille, E. Didelot, T. Mazet, B. Malaman and M. François, *APL Mat.*, 2014, **2**, 124402.
- 43 Y.-L. Hou, G. Xiong, P.-F. Shi, R.-R. Cheng, J.-Z. Cui and B. Zhao, *Chem. Commun.*, 2013, **49**, 6066.
- 44 S.-D. Han, X.-H. Miao, S.-J. Liu and X.-H. Bu, *Inorg. Chem. Front.*, 2014, **1**, 549.
- 45 S.-D. Han, X.-H. Miao, S.-J. Liu and X.-H. Bu, *Chem. Asian J.* 2014, **9**, 3116.
- 46 Y.-C. Chen, L. Qin, Z.-S. Meng, D.-F. Yang, C. Wu, Z. Fu, Y.-Z. Zheng, J.-L. Liu, R. Tarasenko, M. Orendáč, J. Prokleška, V. Sechovský and M.-L. Tong, *J. Mater. Chem. A*, 2014, **2**, 9851.
- 47 E. Palacios, J. A. Rodríguez-Velamazán, M. Evangelisti, G. J. McIntyre, G. Lorusso, D. Visser, L. J. de Jongh, and L. A. Boatner, *Phys. Rev. B*, 2014, **90**, 214423.
- 48 Q. Zhou, F. Yang, D. Liu, Y. Peng, G. Li, Z. Shi and S. Feng, *Inorg. Chem.*, 2012, **51**, 7529-7536.
- 49 K. S. Pedersen, M. A. Sørensen and J. Bendix, *Coord. Chem. Rev.*, 2015, **299**, 1-21.
- 50 M. DiPirro, E. Canavan, P. Shirron and J. Tuttle, *Cryogenics*, 2004, **44**, 559.
- 51 T. E. Katila, V. K. Typpi and G. K. Shenoy, *Solid State Commun.*, 1972, **11**, 1147.
- 52 Y. Yang, Q.-C. Zhang, Y.-Y. Pan, L.-S. Long and L.-S. Zheng, *Chem. Commun.*, 2015, **51**, 7317.

Graphical TOC

The magnetocaloric effect of an inorganic framework material with repeating unit of GdF_3 has been experimentally studied using isothermal magnetization and heat capacity measurements. The maximum entropy change $-\Delta S_{\text{max}}$ reaches $74.8 \text{ J kg}^{-1} \text{ K}^{-1}$ or $528 \text{ mJ cm}^{-3} \text{ K}^{-1}$ for $\Delta H = 9 \text{ T}$ and $T = 1.8 \text{ K}$.

